Iraqi Journal of Physics, 2025 *Vol. 23, No.1, PP. 94-102*

https://doi.org/10.30723/ijp.v23i1.1356 *P-ISSN: 2070-4003*
E-ISSN: 2664-5548

A Preparative (structural) and Spectroscopic Study of Activated Carbon Derived from Date Pits by Calcium Chloride Treatment

Hussein Ali Rahi[1a*] and Nathera Abbas Ali[1b]
[1]*Department of Physics, College of Science, University of Baghdad, Baghdad, Iraq*
[a*]Corresponding author: hussein.Ali2304@sc.uobaghdad.edu.iq

Abstract

This study explores the preparation, structural, and spectroscopic characterization of activated carbon derived from date pits using calcium chloride as an activating agent. Date pits, an abundant agricultural by-product, were processed into activated carbon through chemical activation with varying ratios of calcium chloride. The resulting activated carbon samples were thoroughly analyzed using X-ray Diffraction (XRD), Field Emission Scanning Electron Microscopy (FE-SEM), Fourier-transform Infrared Spectroscopy (FT-IR), and Energy Dispersive X-ray Spectroscopy (EDX). XRD analysis confirmed the presence of crystalline and amorphous carbon phases, with diffraction peaks corresponding to the 101, 110, and 20 planes, indicating successful carbonization and the formation of ordered structures. FE-SEM images showed that pores grew significantly, with pores that were bigger and more noticeable in samples that were activated with higher concentrations of calcium chloride, meaning they had more surface area. FTIR spectra showed increased conjugated C=C double bonds after activation, creating a more porous and chemically active structure. The EDX analysis revealed that the most common elements were carbon and chlorine, suggesting a successful addition of calcium chloride. Other trace elements like phosphorus, sodium, and magnesium were detected, which can be due to the date pits or impurities.

Article Info.

Keywords:
Date Pits, Calcium Chloride, Chemical Activation, Porous Structure, Optical Properties.

Article history:
Received: Aug. 10, 2024
Revised: Dec. 04, 2024
Accepted: Jan. 02, 2025
Published: Mar.01,2025

1. Introduction

Activated carbon, a type of carbon that has been processed to possess a highly porous formation and a substantial surface area, has attracted considerable interest in recent times owing to its diverse range of uses in adsorption, catalysis, and the remediation of environmental issues [1-5]. Among the various sources of raw materials, agricultural residue, due to its plentiful availability, cost-effectiveness, and positive environmental impact, has become a compelling choice as a precursor for the production of activated carbon. Date pits, which are the tough seeds of dates (Phoenix dactylifera), represent one such agricultural byproduct that provides a sustainable and cost-efficient reservoir for the synthesis of activated carbon [6-10]. The process of activation plays a pivotal role in the creation of activated carbon, as it dictates the pore structure, surface area, and chemical characteristics of the material [11, 12]. Chemical activation, impregnating the raw material with activating agents, has been associated with high-surface-area and well-developed porosity-activated carbon [13, 14]. Calcium chloride, $CaCl_2$, among many other activating agents, is preferred due to its good performance in developing the porosity and surface properties of activated carbon. Treatment of date pits with calcium chloride ensures the breaking down of organic components and the creation of pores in the carbon matrix [15-17]. Calcium chloride activates to interact with the date pit biomass, eventually forming micro- and mesopores, which are quite necessary in applications requiring high adsorption capacity. Aside from that, calcium chloride is a dehydrating agent, which creates

conditions for the removal of volatile components and additionally promotes the formation of the carbon structure [18-22]. Apart from the preparative advantages, calcium chloride in activated carbon production has a significant effect on the chemical and physical properties of the material, which can be fully characterized by various spectroscopic techniques such as Fourier-transform infrared spectroscopy, field emission scanning electron microscopy analysis, energy dispersive X-ray spectroscopy analysis, and X-ray diffraction [23-29].

This study aims to explore the potential of date pits as a raw material for activated carbon production, focusing on the effects of calcium chloride treatment on the structural and spectroscopic properties of the resulting carbon. By investigating the activation process and characterizing the material using advanced spectroscopic techniques, this research seeks to contribute to the development of high-performance activated carbon from renewable resources.

2. Experimental Work

In this work, date pits, which are hard seeds, of different sizes were chosen to prepare activated carbon using calcium chloride treatment. After separating, the pits from the fruits, the pits were washed thoroughly with distilled water. The cleaned pits were dried at 60°C in an oven for 24 hours to remove the water content. The dried date pits were finely ground to a powder and taken as the main raw material to be treated. This powdered material was transferred into a ceramic vessel; calcium chloride was mixed with the powdered pits in a ratio of 0.5:1 to 1.5:1 with an increment of 0.5% calcium chloride in each batch. For proper agitation, 10 ml of distilled water was added to the mixture, which was later homogenized. The homogenized mixture was subjected to a two-step heating process. First, it was heated to 400°C in an oven for three hours to start activating it. Second, it was reheated at 600°C for two hours more for the complete activation of carbon. Then, after heating, the samples were left to cool naturally at room temperature. The samples were washed a few times with distilled water until the pH of the wash water became neutral(pH=7.51) to ensure that all residual calcium chloride was removed from the activated carbon. Subsequently, the activated carbon samples were dried at 60°C for 48 hours inside an Acupetter Oven. The steps of this process are illustrated in Fig. 1.

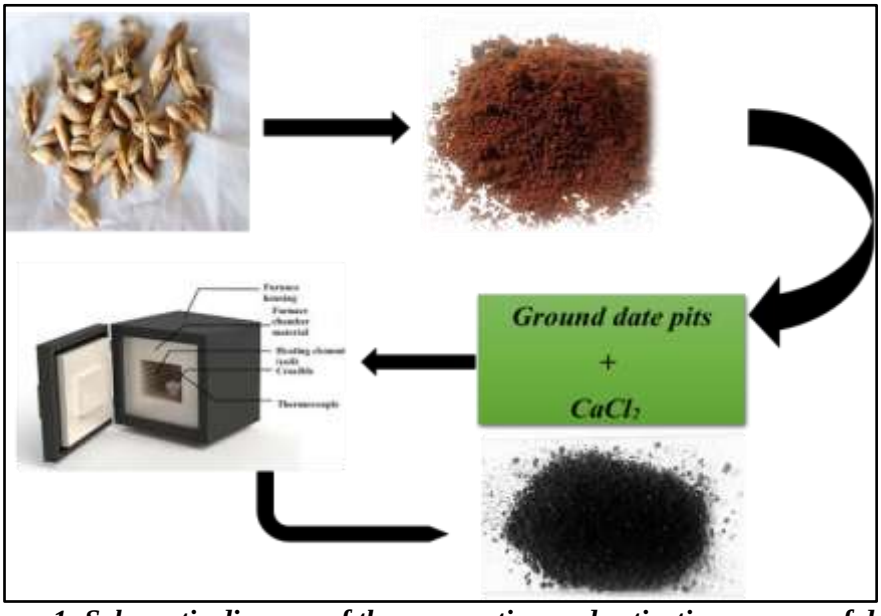

Figure 1: Schematic diagram of the preparation and activation process of date pits to prepare activated carbon using calcium chloride treatment.

Three different activated carbon samples were prepared with varying the concentrations of calcium chloride as follows: the first one, labeled AC1, was prepared with a calcium chloride to date pit ratio of 0.5:1, the second sample (AC2) used a ratio of 1:1, and the third one (AC3) was prepared with a ratio of 1.5:1. Data for these samples are given in Table 1.

Table 1: Overview of the Three Varieties of Activated Carbon.

Date Pits	Calcium Chloride ($CaCl_2$)	Model
1 g	0.5 g	AC1
1 g	1 g	AC2
1 g	1.5 g	AC3

3. Results and Discussion

3. 1. XRD Spectra Analysis

The existence of carbon crystal structures in the activated carbon samples was confirmed through the observed X-ray diffraction patterns, consistent with the standard JCPDS profile 96-901-1641. The different diffraction peaks identified correspond to carbon crystal lattice planes (101), (110), and (20$\bar{1}$); thus, indicating well-defined crystalline carbon structures. As shown in Fig.2, the ratios of calcium chloride used during the activation may further have some effects on the degree of crystallinity and the extent of the existing amorphous carbon in the activated carbon samples. X-ray diffraction patterns showed that crystalline and amorphous phases of carbon are present in the activated carbon samples. The peaks pointed out the ordered formation of carbon structures, while zones that lacked well-defined structures reflected amorphous carbon. This balance of crystalline and amorphous phases can be explained by the different ratios of calcium chloride used, which change the global crystallinity and other structural characteristics of activated carbon.

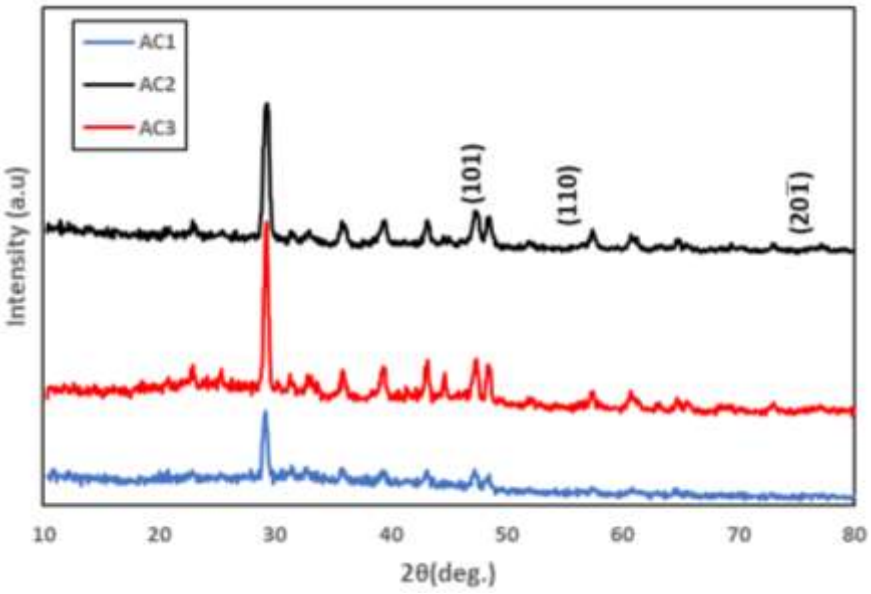

Figure 2: XRD spectra of activated carbon samples AC1, AC2, and AC3.

3. 2. FE-SEM Analysis

In this work, Field Emission Scanning Electron Microscopy (FE-SEM) was used to further investigate the surface morphology of the activated carbon samples. The detailed surface features for the samples are shown in Fig. 3(a, b, c), where many big pores covered the surface of the activated carbon. A closer look at Fig.3b and c shows

that these pores are more evident in samples AC2 and AC3. Their prominence in these samples can be attributed to the higher ratios of calcium chloride used during the activation process. In FE-SEM, the pores appeared due to the higher proportions of calcium chloride because the calcium chloride that contributed to the development of the pores was burned with the raw material during the carbonization process, while the remaining that was not burned was removed during washing. Calcium chloride acts as a dehydrating agent and facilitates the formation of larger pores by promoting the removal of volatile compounds and the breakdown of the carbonaceous material. This leads to the development of an extensive porous network. However, the presence of substantial material debris within these pores, as observed in the images, suggests that some unreacted residues or by-products from the activation process have not been entirely removed. This debris may result from incomplete combustion or residual precursor material that has not been entirely converted during the activation stages. Overall, the FE-SEM analysis not only highlights the surface porosity but also provides insights into the effectiveness of the activation process.

Complete removal of residual material is crucial for optimizing the performance of activated carbon in various applications. By examining the surface morphology and pore structure and identifying any residues or non-activated regions through FE-SEM imaging, it is possible to demonstrate the effectiveness of the activation process and the residual material removal. This evidence would be crucial for optimizing the activation process, ensuring the activated carbon's optimal performance in various applications like adsorption, catalysis, or filtration. Additionally, supplementary techniques like EDX surface area analysis can help confirm these observations and provide further insight into the material's properties.

Calcium chloride enhances the chemical reaction that leads to the opening of pores in the carbon structure, which increases the volume of the fine pores in the activated carbon. These pores contribute to an increase in the surface area of the activated carbon. Despite the increase in porosity, there may be a slight reduction in the total volume of the particles themselves due to the partial breakdown of the carbon structure.

3. 3. EDX Analysis

Fig. 4 shows EDX analysis of the activated carbon samples AC1, AC2 and AC3. EDX analysis details the elemental composition in the samples. The data showed that carbon, C, formed the highest percentage of the samples, which is expected since the main raw material is date pits, mainly composed of carbon. The presence of oxygen can be attributed to chemical bonds that stabilize the carbon atoms and residual moisture remaining in the samples after activation. Chlorine was present in the samples, thus representing the successful incorporation of calcium chloride during activation. In EDX testing, very small amounts of Ca and Cl were detected, which can be attributed to the mixtures. It simply means some chlorine was either chemically bonded to the carbon or remained entrapped in such pores that were formed through activation. There was also calcium, Ca, directly from the activating reagent used, which is calcium chloride. The calcium might have complexed/bonded to the carbon matrix or still remained as residues of the starting material. The trace amounts of P, Na, and Mg detected were likely due to their natural presence in date pits or probably from some impurities of the materials used during preparation. On the whole, EDX analysis confirmed the incorporation of activation agents and provided information on the elemental composition and probable impurities in the activated carbon samples.

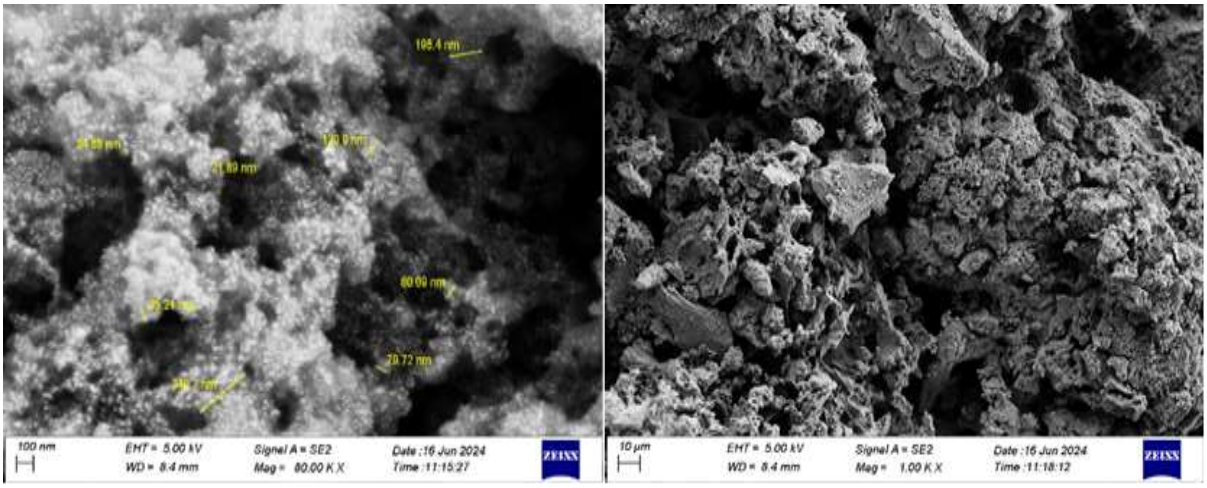

(a)

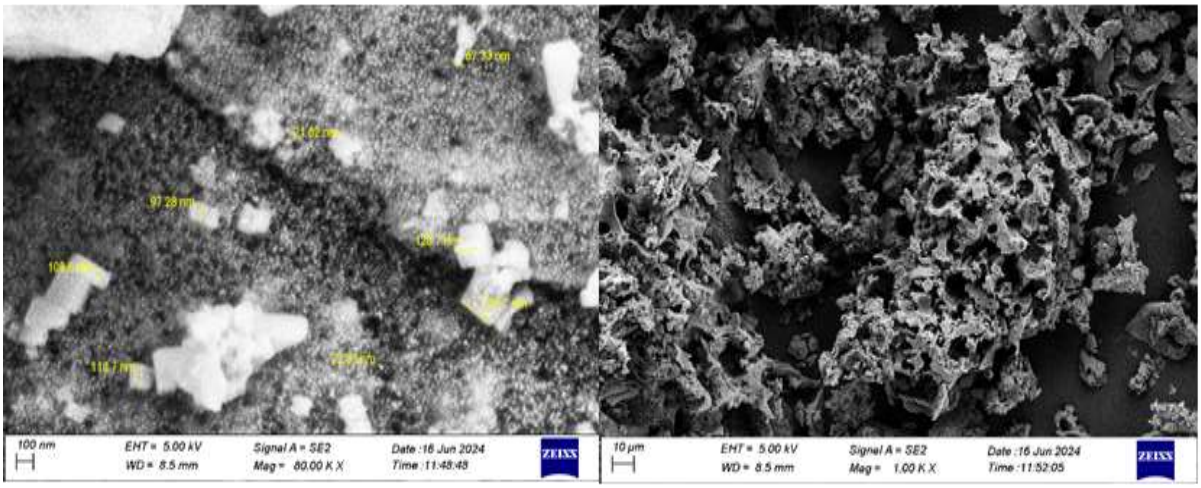

(b)

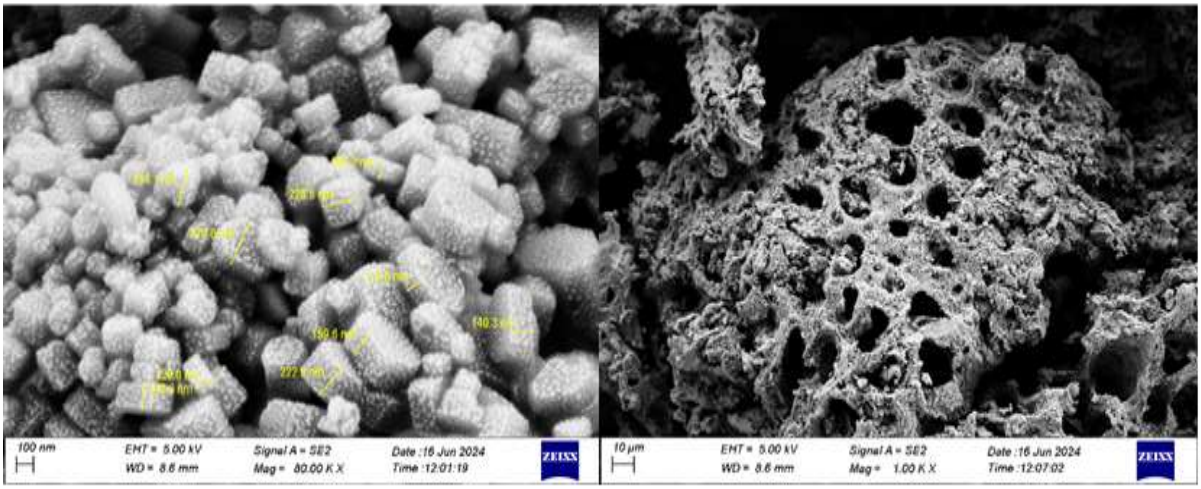

(c)

Figure 3: FE-SEM images of activated carbon samples (a) AC1, (b) AC2, and (c) AC3.

Table 1. Elemental Composition via EDX Analysis of the Sample (AC1).

Spectrum 1				
Element	**Line Type**	**Weight %**	**Weight % Shigma**	**Atomic %**
C	K series	34.96	0.83	51.87
O	K series	26.96	0.62	30.02
Cl	K series	15.65	0.27	7.87
P	K series	21.16	0.35	9.41
P	K series	0.70	0.08	0.40
Na	K series	0.39	0.07	0.30
Mg	K series	0.18	0.05	0.13
Total		100.00		100.00

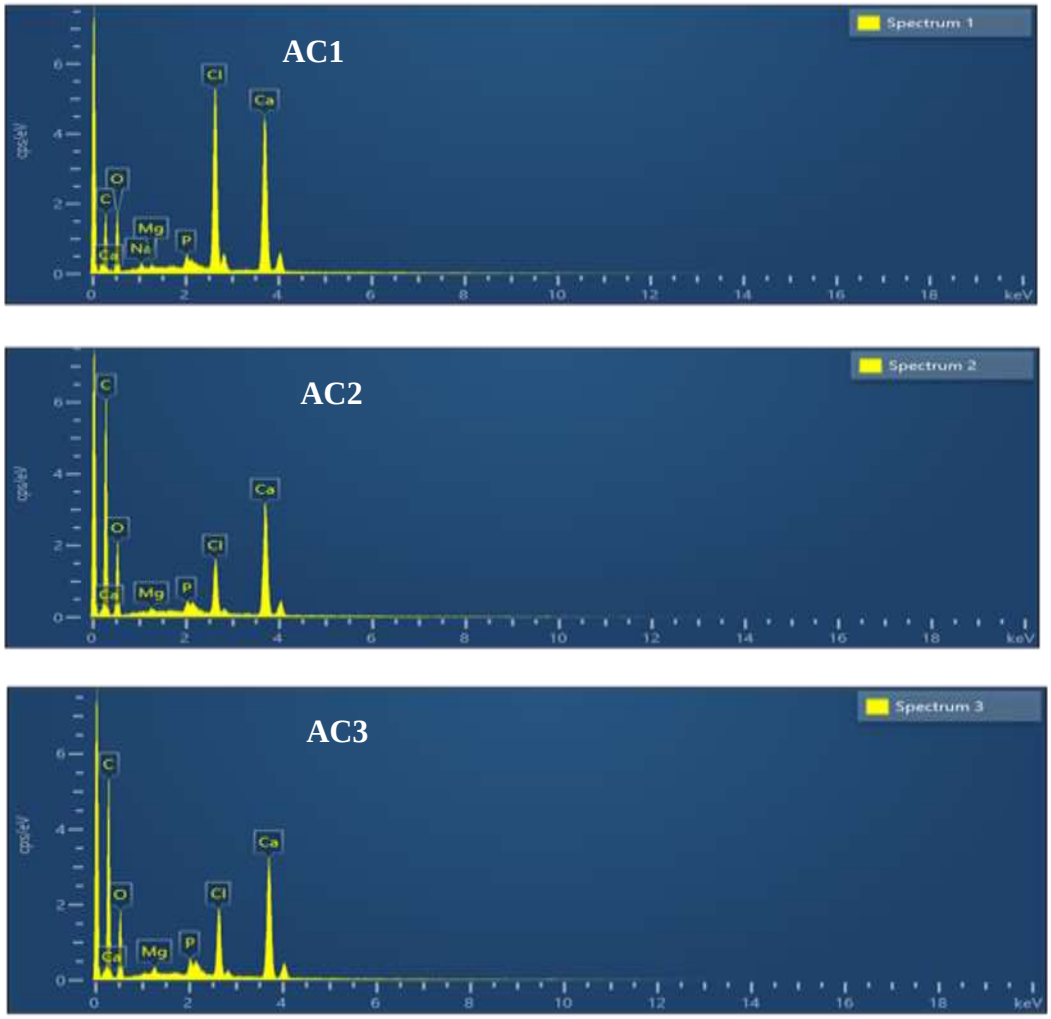

Figure 4: EDX spectra of activated carbon samples AC1, AC2, and AC3.

Table 2. Elemental Composition via EDX Analysis of the Sample (AC2).

Spectrum 1				
Element	**Line Type**	**Weight %**	**Weight % Shigma**	**Atomic %**
C	K series	55.08	0.53	68.22
Cl	K series	4.16	0.10	1.75
Ca	K series	13.54	0.21	5.02
O	K series	26.51	0.54	24.65
P	K series	0.55	0.06	0.26
Mg	K series	0.16	0.04	0.10
Total		100.00		100.00

Table 3. Elemental Composition via EDX Analysis of the Sample (AC3).

Spectrum 1				
Element	**Line Type**	**Weight %**	**Weight % Shigma**	**Atomic %**
C	K series	54.68	0.56	68.47
Cl	K series	5.13	0.12	2.18
Ca	K series	14.06	0.22	5.28
Mg	K series	0.36	0.05	0.22
P	K series	0.83	0.07	0.40
O	K series	24.94	0.55	23.45
Total		100.00		100.00

3. 4. FT-IR Analysis

Fig. 5 presents the FT-IR spectra of the activated carbon samples AC1, AC2, and AC3. The data revealed several key functional groups and chemical bonds that provide insight into the structural and chemical composition of the activated carbon. A very prominent peak within the 3500-3200 cm^{-1} wavenumber region can be associated with the O-H stretching vibration of alcohol and phenol functional groups. This O-H stretch could be due to either residual water molecules trapped in the carbon matrix or due to hydroxyl groups bonded directly on the surface of the carbon. This bond indicates incomplete drying or side reactions that have occurred during the activation process. An increase in absorption intensity within the 1500-1350 cm^{-1} region would indicate a higher concentration of conjugated C=C bonds. Therefore, this increase in absorption means that the activation process has successfully increased the surface area of the carbon structure. These changes may also broaden or split the shape of the band due to changes in the chemical environment of the C=C bonds. These changes could have been caused by interactions with calcium chloride or new compound formation during activation. The peak at 873.753 cm^{-1} can be related to the stretching of the C-C bond of the aromatic ring or the out-of-plane bending of the C-H bond of such rings. This peak shows the graphitic structure that is present in the activated carbon. This graphitic structure indicates that the carbonization process has been successful and highly ordered carbon domains have been formed, which can enhance conductivity and adsorption ability. More importantly, FT-IR analysis describes the chemical composition and structural changes in activated carbon that give insights into the effectiveness of activation and the resulting material properties.

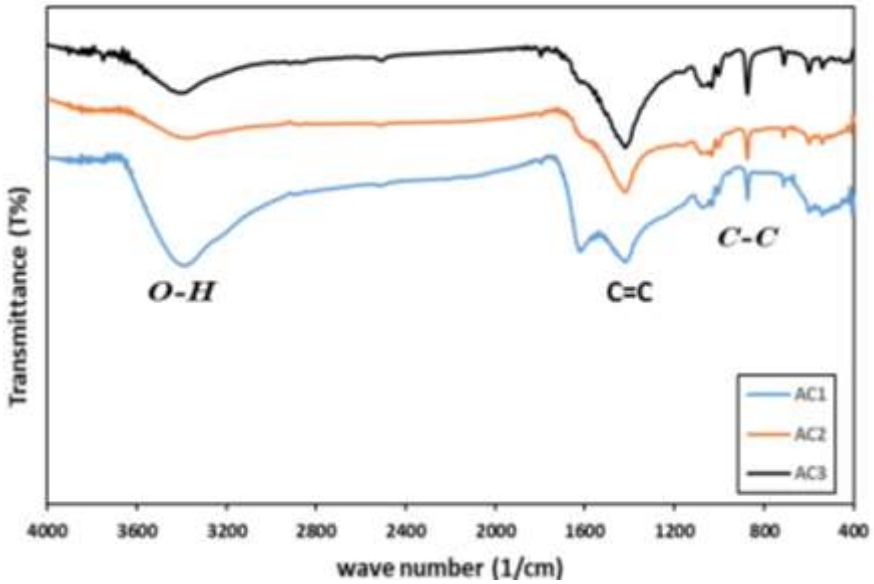

Figure 5: FT-IR spectra of activated carbon samples AC1, AC2, and AC3.

4. Conclusions

Calcium chloride effectively converted date pits into valuable activated carbon. FE-SEM results showed a drastic change in pore structure and surface area increment for activated carbon produced with increasing concentrations of $CaCl_2$. The FT-IR results showed that conjugated carbon-carbon double bonds (C=C) increased. This indicates that the surface area grew and pores formed. EDX analysis showed that carbon was the main element, proving calcium chloride worked well during activation. The activated carbon produced from this process showed commendable characteristics, such as water purification, gas adsorption, and storage.

Conflict of Interest

The authors declare no conflict of interest.

References

1. G. Sharma, S. Sharma, A. Kumar, C. W. Lai, M. Naushad, Shehnaz, J. Iqbal, F. J. Stadler, and C. A. Igwegbe, Adsorp. Sci. Tech. **2022**, 4184809 (2022). DOI: 10.1155/2022/4184809.
2. R. Chakraborty, V. K, M. Pradhan, and A. K. Nayak, J. Mater. Chem. A **10**, 6965 (2022). DOI: 10.1039/D1TA10269A.
3. B. S. Rathi, T. M, K. S. S, G. R, and R. V, Envir. Qual. Manag. **33**, 907 (2024). DOI: 10.1002/tqem.22166.
4. M. Mariana, A. K. H.P.S, E. M. Mistar, E. B. Yahya, T. Alfatah, M. Danish, and M. Amayreh, J. Water Proce. Eng. **43**, 102221 (2021). DOI: 10.1016/j.jwpe.2021.102221.
5. A. B. D. Nandiyanto, S. N. Hofifah, H. T. Inayah, S. R. Putri, S. S. Apriliani, S. Anggraeni, D. Usdiyana, and D. Usdiyana, Iraqi J. Sci. **62**, 1404 (2021). DOI: 10.24996/ijs.2021.62.5.2.
6. Y. A. Mahmood and B. T. Chiad, Iraqi J. Phys. **18**, 62 (2020). DOI: 10.30723/ijp.v18i44.510.
7. R. F. Kadhim, Iraqi J. Phys. **15**, 11 (2019). DOI: 10.30723/ijp.v15i33.135.
8. D. E. Al-Mammar, Iraqi J. Sci. **65**, 3606 (2024). DOI: 10.24996/ijs.2024.65.7.3.
9. M. Azam, S. M. Wabaidur, M. R. Khan, S. I. Al-Resayes, and M. S. Islam, Polymers **14**, 914 (2022). DOI: 10.3390/polym14050914.
10. R. Krishnamoorthy, B. Govindan, F. Banat, V. Sagadevan, M. Purushothaman, and P. L. Show, J. Biosci. Bioeng. **128**, 88 (2019). DOI: 10.1016/j.jbiosc.2018.12.011.
11. P. Feng, J. Li, H. Wang, and Z. Xu, ACS Omega **5**, 24064 (2020). DOI: 10.1021/acsomega.0c03494.
12. Y. Gao, Q. Yue, B. Gao, and A. Li, Sci. Tot. Envir. **746**, 141094 (2020). DOI: 10.1016/j.scitotenv.2020.141094.
13. E. M. Mistar, T. Alfatah, and M. D. Supardan, J. Mat. Res. Tech. **9**, 6278 (2020). DOI: 10.1016/j.jmrt.2020.03.041.
14. M. Şirazi and S. Aslan, Chem. Eng. Communic. **208**, 1479 (2021). DOI: 10.1080/00986445.2020.1864628.
15. C. Bouchelta, M. S. Medjram, O. Bertrand, and J.-P. Bellat, J. Analyt. Appl. Pyroly. **82**, 70 (2008). DOI: 10.1016/j.jaap.2007.12.009.
16. M. Auta and B. H. Hameed, Chem. Eng. J. **171**, 502 (2011). DOI: 10.1016/j.cej.2011.04.017.
17. B. Jin, K. Jing, J. Liu, X. Zhang, and G. Liu, J. Analy. Appl. Pyroly. **125**, 117 (2017). DOI: 10.1016/j.jaap.2017.04.010.
18. K. Gergova and S. Eser, Carbon **34**, 879 (1996). DOI: 10.1016/0008-6223(96)00028-0.
19. Q. Touloumet, L. Silvester, L. Bois, G. Postole, and A. Auroux, Sol. Ener. Mat. Sol. Cells **231**, 111332 (2021). DOI: 10.1016/j.solmat.2021.111332.
20. A. Shukla and A. Kumar, Separat. Purific. Tech. **41**, 83 (2005). DOI: 10.1016/j.seppur.2004.05.001.
21. T. Ando, A. Mori, R. Ito, and K. Nishiwaki, J. Anesth. **31**, 911 (2017). DOI: 10.1007/s00540-017-2397-0.
22. I. Okman, S. Karagöz, T. Tay, and M. Erdem, Appl. Surf. Sci. **293**, 138 (2014). DOI: 10.1016/j.apsusc.2013.12.117.
23. B. S. Girgis and A.-N. A. El-Hendawy, Micropor. Mesopor. Mat. **52**, 105 (2002). DOI: 10.1016/S1387-1811(01)00481-4.
24. O. A. Hussain, A. S. Hathout, Y. E. Abdel-Mobdy, M. M. Rashed, E. A. Abdel Rahim, and A. S. M. Fouzy, Toxicol. Rep. **10**, 146 (2023). DOI: 10.1016/j.toxrep.2023.01.011.
25. M. W. Khaled, A. A. Beddai, and A. M. N. Almohaisen, AIP Conf. Proc. **3105**, 060012 (2024). DOI: 10.1063/5.0212411.

26. W. Ahmad, S. Qaiser, R. Ullah, B. Mohamed Jan, M. A. Karakassides, C. E. Salmas, G. Kenanakis, and R. Ikram, Materials **14**, 34 (2021). DOI: 10.3390/ma14010034.
27. E. H. Sujiono, D. Zabrian, Zurnansyah, Mulyati, V. Zharvan, Samnur, and N. A. Humairah, Res. Chem. **4**, 100291 (2022). DOI: 10.1016/j.rechem.2022.100291.
28. A. M. Jasim and N. Abbas Ali, Def. Diffus. For. **425**, 85 (2023). DOI: 10.4028/p-8uh5h0.
29. A. M. Jasim and N. A. Ali, AIP Conf. Proc. **2922**, 040011 (2024). DOI: 10.1063/5.0185116.

دراسة تحضيرية (بنيوية) وطيفية للكربون المنشط المشتق من نوى التمر عن طريق المعالجة بكلوريد الكالسيوم

حسين علي راهي[1] ونذيرة عباس علي[1]
[1] قسم الفيزياء، كلية العلوم، جامعة بغداد، بغداد، العراق

الخلاصة

تتناول هذه الدراسة التحضير والتوصيف الطيفي للكربون المنشط المشتق من نواة التمر باستخدام كلوريد الكالسيوم كعامل منشط. تمت معالجة نواة التمر، وهو منتج ثانوي زراعي وفير، إلى كربون منشط من خلال التنشيط الكيميائي بنسب متفاوتة من كلوريد الكالسيوم. تم تحليل عينات الكربون المنشط الناتجة بدقة باستخدام حيود الأشعة السينية(XRD) ، والمجهر الإلكتروني لمسح الانبعاثات الميدانية (FE-SEM)، والتحليل الطيفي للأشعة تحت الحمراء لتحويل فورييه (FT-IR)، والتحليل الطيفي للأشعة السينية المشتتة من الطاقة (EDX). أكد تحليل XRD وجود كل من مراحل الكربون البلورية وغير المتبلورة، مع قمم الحيود المقابلة للمستويات (101)، (110)، و$(20\bar{1})$، مما يشير إلى الكربنة الناجحة وتشكيل الهياكل المنظمة .كشفت صور FE-SEM عن تطور كبير في المسام، مع تنشيط المسام الأكبر والأكثر وضوحًا في العينات بتركيزات أعلى من كلوريد الكالسيوم، مما يعكس مساحة سطحية محسنة. أظهر التحليل الطيفي (FT-IR) زيادة في الروابط المزدوجة بين الكربون والكربون (C=C) بعد التنشيط، مما يؤكد نجاح إنشاء بنية أكثر مسامية ونشط كيميائيًا .أشار تحليل EDX إلى أن الكربون كان العنصر السائد، مع وجود الكلور مما يؤكد الدمج الفعال لكلوريد الكالسيوم. بالإضافة إلى ذلك، تم الكشف عن العناصر النزرة مثل الفوسفور والصوديوم والمغنيسيوم، والتي من المحتمل أن يكون مصدرها نواة التمر أو الشوائب.

الكلمات المفتاحية: نوى التمر، كلوريد الكالسيوم، التنشيط الكيميائي، التركيب المسامي، الخواص البصرية.